

Production of Light Nuclei in Au+Au Collisions with the STAR BES-II Program

Yixuan Jin^{1,*} (For the STAR Collaboration)

¹Institute of Particle Physics and Key Laboratory of Quark & Lepton Physics (MOE),
Central China Normal University, Wuhan, 430079, China.

Abstract. The yields and ratios of light nuclei in heavy-ion collisions offer a method to distinguish between the thermal and coalescence models. Ratios such as $N_t \times N_p / N_d^2$ and $N_{^3\text{He}} \times N_p / N_d^2$ are suggested as potential probes to investigate critical phenomena within the QCD phase diagram. The significantly larger datasets from STAR BES-II compared to BES-I, combined with enhanced detector capabilities, allow for more precise measurements. In this proceeding, we present the centrality and energy dependence of transverse momentum spectra and particle yields of (anti-)proton, (anti-)deuteron, and ^3He at BES-II energies ($\sqrt{s_{\text{NN}}} = 7.7 - 27$ GeV), as well as the light nuclei to proton yield ratios and coalescence parameters ($B_2(\text{d})$ and $B_3(^3\text{He})$).

1 Introduction

In the framework of Quantum Chromodynamics (QCD), elementary particles are confined within hadrons at low temperatures and baryon densities. Conversely, at higher temperatures or/and high baryon densities, hadronic matter transitions into quark-gluon plasma (QGP), where the dominate degrees of freedom are quarks and gluons. Experimentally, as the initial temperature (T) and the baryon chemical potential (μ_B) vary with the center-of-mass collision energy, the phase diagram can be explored by adjusting the beam energy [1–3].

The Beam Energy Scan (BES) program at the Relativistic Heavy-Ion Collider (RHIC) aims to investigate QGP signatures, understand the nature of the phase transition, and identify the conjectured critical point. The second phase of the Beam Energy Scan (BES-II), with about 10 times more data than the BES-I phase and enhanced detector capabilities, is driven by the need for more precise experimental results allowing more firm physics conclusions.

Based on the coalescence model, the light nuclei compound ratios such as $N_t \times N_p / N_d^2$ and $N_{^3\text{He}} \times N_p / N_d^2$ are sensitive to the neutron density fluctuations, therefore, the ratios have been suggested as a potential probe to search for the critical phenomena in the QCD phase diagram [4]. The light nuclei production in Au+Au collisions has been measured by the STAR BES-I and fixed-target program [5–7].

In this proceeding, we present the transverse momentum spectra, particle yields, and yield ratios for light nuclei in Au+Au collisions at $\sqrt{s_{\text{NN}}} = 7.7 - 27$ GeV from the STAR BES-II program. Light nuclei to proton yield ratios decrease with increasing collision energy. Furthermore, the coalescence parameters ($B_2(\text{d})$ and $B_3(^3\text{He})$) demonstrate centrality and p_T dependence, indicating the influence of collective expansion.

*e-mail: jyx@mails.ccnuc.edu.cn

38 2 Analysis details

39 Particles are identified using the Time Projection Chamber (TPC) at low p_T , with Time of
 40 Flight (TOF) added at higher p_T . After signal extraction, the spectra are corrected for energy
 41 loss, TPC tracking efficiency, TOF matching efficiency, and knock-out effects specifically for
 42 protons and deuterons. The feed-down contributions of proton and anti-proton from the weak
 43 decay of strange baryons are also applied.

44 Point-to-point systematic uncertainties on the spectra are estimated by varying track se-
 45 lection and analysis cuts. The systematic uncertainties of dN/dy are assessed by consid-
 46 ering the point-to-point uncertainties in spectra, and the extrapolated range from the spec-
 47 tra fitting by examining the deviation between the Blast-Wave model fit and the double- p_T
 48 ($p_0 e^{-p_T^2/p_1^2} + p_2 e^{-p_T^2/p_3^2}$) function.

49 3 Results

50 3.1 Corrected transverse momentum spectra

51 The transverse momentum (p_T) spectra of deuterons and ^3He in Au+Au collisions from
 52 the STAR BES-II program are shown in Fig. 1. Due to higher statistics, the BES-II spectra
 53 cover more centrality bins, and remain consistent with those from BES-I within the uncer-
 54 tainties. Additionally, thanks to the inner TPC (iTPC), the p_T acceptance is significantly
 55 enhanced, and the extended p_T ranges in BES-II contribute to a reduction in the systematic
 56 uncertainties of the particle yields.

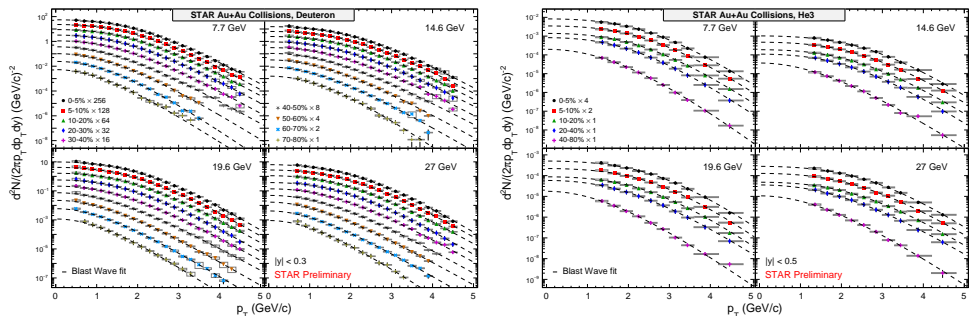


Figure 1. The transverse momentum spectra of deuteron (left) and ^3He (right) at mid-rapidity (with $|y| < 0.3$ for deuteron and $|y| < 0.5$ for ^3He) for different centrality bins in Au+Au collisions from the STAR BES-II program. The dashed lines represent the corresponding Blast-Wave fits. Statistical and systematic uncertainties are indicated by vertical lines and boxes, respectively.

57 3.2 Particle Yields

58 The particle yields (dN/dy) are extracted from p_T spectra, with measurement ranges in-
 59 tegrated over p_T and extrapolations carried out using Blast-Wave model fits. Figure 2 shows
 60 dN/dy for different particles with the scaling of their corresponding spin degeneracy factor
 61 $2J + 1$. These scaled yields of light nuclei follow an exponential distribution of the form
 62 p_0/P^{A-1} , where P is the penalty factor determined by the Boltzmann factor $e^{(m_N - \mu_B)/T}$ in
 63 the thermal model. The penalty factor increases with higher beam energy, indicating that it be-
 64 comes more challenging to form high-mass objects.

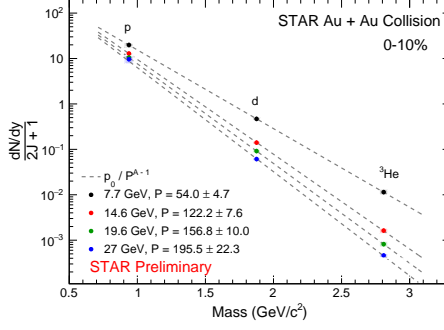


Figure 2. The mass m_A (where A is the mass number) dependence of dN/dy for protons, deuterons, and ${}^3\text{He}$, scaled by the spin degeneracy factor $2J + 1$, is shown for Au+Au collisions at BES-II energies of $\sqrt{s_{\text{NN}}} = 7.7 - 27$ GeV. Statistical uncertainties are indicated by vertical lines, while systematic uncertainties are shown by boxes. The yields are fitted using dashed lines representing exponential functions.

65 3.3 Particle Yield Ratios

66 Figure 3 presents the light nuclei to proton yield ratios, which are consistent with BES-I
 67 results within uncertainties. Both the N_d/N_p and $N_{{}^3\text{He}}/N_p$ ratios decrease monotonically with
 68 increasing collision energy, and the difference between these two ratios becomes smaller at
 69 lower energies. The thermal model, shown by dashed lines, describes the N_d/N_p ratios well,
 70 but it overestimates the N_t/N_p and $N_{{}^3\text{He}}/N_p$ ratios by a factor of about 2, likely due to the
 71 effects of hadronic re-scattering during the hadronic expansion stage.

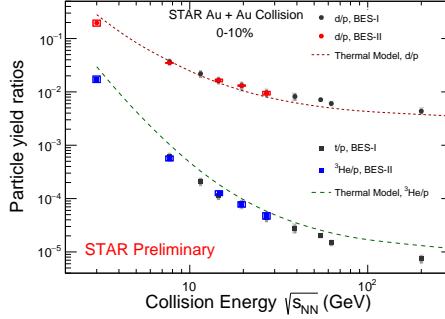


Figure 3. The energy dependence of N_d/N_p (the red circles) and $N_{{}^3\text{He}}/N_p$ (the blue squares) in the most central 0-10% collisions from BES-II. The gray points represent N_d/N_p and N_t/N_p from BES-I. Vertical lines and boxes represent statistical and systematic uncertainties, respectively. The lines show the light nuclei to proton yield ratios from the thermal model.

72 3.4 Coalescence Parameters

73 In the coalescence picture:

$$E_A \frac{d^3 N_A}{dp_A^3} = B_A \left(E_p \frac{d^3 N_p}{dp_p^3} \right)^Z \left(E_n \frac{d^3 N_n}{dp_n^3} \right)^{A-Z} \approx B_A \left(E_p \frac{d^3 N_p}{dp_p^3} \right)^A \quad (1)$$

74 where A is the mass number and Z is the charge number of the light nucleus. p_n, p_p, p_A are
 75 the momenta of the neutron, proton, and nucleus.

76 The invariant yield of light nuclei is proportional to the invariant yield of nucleons, with
 77 the coalescence parameter B_A reflecting the probability of nucleon coalescence and relating
 78 to the local nucleon density. Figure 4 shows coalescence parameters as a function of p_T/A
 79 across different centralities. B_A increases with transverse momentum, suggesting an expanding
 80 collision system, and also increases from central to peripheral collisions, likely due to a
 81 decreasing source volume.

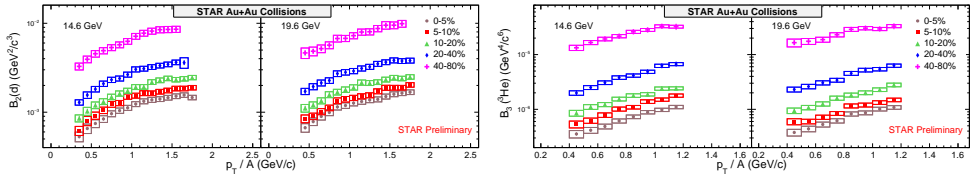


Figure 4. Number of constituent nucleon (NCN) scaling for p_T dependence of B_2 for deuteron (left) and B_3 for ${}^3\text{He}$ (right) in centrality 0-5%, 5-10%, 10-20%, 20-40% and 40-80% in Au+Au collisions at $\sqrt{s_{\text{NN}}} = 14.6$ and 19.6 GeV. The boxes represent the systematic uncertainties.

82 4 Conclusions

83 The production of primordial proton, deuteron, and ${}^3\text{He}$ in Au+Au collisions at $\sqrt{s_{\text{NN}}} =$
 84 7.7 – 27 GeV from RHIC STAR BES-II is reported in these proceedings. The particle ratios
 85 N_d/N_p and $N_{{}^3\text{He}}/N_p$ show a monotonic decrease with collision energy. The thermal model
 86 over-predicts N_d/N_p and $N_{{}^3\text{He}}/N_p$ by a factor of about 2. The coalescence parameter B_A
 87 increase from low to high p_T due to collective expansion, and decreasing source volume
 88 results in a rise of B_A from central to peripheral collisions.

89 5 Acknowledgement

90 This work was supported by National Key Research and Development Program of
 91 China (No.2022YFA1604900, No.2020YFE0202002), National Natural Science Foundation
 92 of China (No.12122505) and the Fundamental Research Funds for the Central Universities
 93 (CCNU220N003).

94 References

- 95 [1] A. Bzdak, S. Esumi, V. Koch, J. F. Liao, M. Stephanov, N. Xu. Phys. Rep. **853**, 1-87
 96 (2020).
 97 [2] X. F. Luo, Q. Wang, N. Xu, P. F. Zhuang, *Properties of QCD matter at high baryon*
 98 *density* (Springer, Singapore, 2022) 1-75
 99 [3] J. H. Chen, X. Dong, X. H. HE, H. Z. Huang, F. Liu *et al.* arXiv:2407.02935[nucl-ex].
 100 [4] K. J. Sun, L. W. Chen, C. M. Ko, Z. B. Xu. Phys. Lett. B. **774**, 103-107 (2017).
 101 [5] J. Adam *et al.* [STAR Collaboration]. Phys. Rev. C 99 (2019) 6, 064905.
 102 [6] M. I. Abdulhamid *et al.* [STAR Collaboration]. Phys. Rev. Lett. 130 (2023) 202301.
 103 [7] STAR Collaboration. arXiv:2311.11020[nucl-ex].